SAND2018-0961J

Double Sided Grating Fabrication for High Energy X-Ray Phase Contrast Imaging

Andrew E. Hollowell[1*], Christian L. Arrington[1], Patrick Finnegan[1], Kate Musick[1], Paul Resnick[1], Steve Volk[1], Amber Dagel[1]

1 - Sandia National Laboratories, 1515 Eubank BLVD SE, Albuquerque, NM 87123
* corresponding author: Andrew E. Hollowell – aehollo@sandia.gov

Keywords: XPCI, Silicon Deep Reactive Ion Etch, Front-to-back alignment, gratings, electrocoating, conformal plating

Abstract

State of the art grating fabrication currently limits the maximum source energy that can be used in lab based x-ray phase contrast imaging (XPCI) systems. In order to move to higher source energies, and image high density materials or image through encapsulating barriers, new grating fabrication methods are needed. In this work we have analyzed a new modality for grating fabrication that involves precision alignment of etched gratings on both sides of a substrate, effectively doubling the thickness of the grating. We have achieved a front-to-backside feature alignment accuracy of 0.5 µm demonstrating a methodology that can be applied to any grating fabrication approach extending the attainable aspect ratios allowing higher energy lab based XPCI systems.

Introduction

A three-grating laboratory XPCI system relies on: a source grating, a phase grating, and an analyzer grating. Traditionally, XPCI gratings are fabricated using a LIGA approach in which an organic template is patterned and then filled with electrodeposited gold (Au) using a through-mask plating approach [1]. The researchers at Karlsruher Institute for Technology have led the advancement and application of LIGA for XPCI gratings by developing approaches for realizing aspect ratios as high as 100:1 [1] and large areas by scanning a resist coated substrate through a masked synchrotron beam [2]. While both extreme aspect ratios and large areas have been realized with LIGA based fabrication, they have not been able to achieve them both at the same time due to the mechanical limitations of a 1D organic template. High aspect ratios are limited to smaller areas, tens of cm^2, and achieved by inserting lateral support structures in the grating. These lateral support structures add distortion in the final image and limit the photon throughput. The large area LIGA gratings are limited in aspect ratios because the organic template is not structurally sound enough to support a true 1D grating over large distances.

In exploration of a technique capable of obtaining both a large field of view (large area grating) and high aspect ratios, researchers have branched beyond LIGA and explored alternative materials to be used as templates in place of organic resist. The most commonly used alternative to x-ray exposed resist has been silicon (Si) [3,4,5]. Once the silicon template is formed it is

then coated with a high absorbing material through angled evaporation [4], precision electroplating [5], or embossing [3]. A variety of techniques have been used to create these Si templates including anisotropic KOH etching of Si, metal assisted chemical etching (MACE) [6], and deep reactive ion etching (DRIE) [5]. Each of these Si etching techniques have their advantages and disadvantages. KOH etching is capable of obtaining extreme aspect ratios due to the high selectivity in etch rates of different crystalline planes; however, the etch mask must be precisely aligned to a specific crystalline plane (within 0.1°), which is difficult to achieve [7,8]. MACE has been proven to obtain extremely high aspect ratios without the need to align to a specific crystal plane, however it is difficult to control the uniformity of the etch depth and grating uniformity across a large area. DRIE can achieve both large areas and very high uniformity across a full wafer; however, the aspect ratio is limited by RIE lag [9]. RIE lag can be reduced with cryogenic DRIE, increasing the achievable etch depths, but it is still inherently limited.

Regardless of which grating fabrication method is used there will always be an inherent limit in the thickness of the exposed organic template or alternatively in the etch depth of the Si grating. In order to de-couple limits on the thickness of the grating template from the self-limiting etch processes, we investigated methods for aligning gratings on both the front and backsides of a substrate. Successful front-to-backside alignment effectively doubles the thickness of the grating, independent of the technique used to etch the Si template. Doubling the thickness of the grating opens up the possibility of using cheaper absorbing materials, such as embossing with AuSn [3], or Pb based solder and still obtaining the same absorption contrast. Continuing to use a high absorbing material while doubling the thickness of the grating will increase the contrast obtained when moving to higher x-ray source energies. Due to the feature sizes of these gratings, precision front-to-back alignment is difficult to achieve and depends on precision microelectronics lithography tools. Fabricating high aspect ratio features on both sides of the grating is also difficult to achieve due to the need to temporarily protect one side of the grating while processing on the opposite side of the substrate. After both sides are processed, this temporary support material must be removed without damaging the gratings on either side of the substrate. Further, quantitatively measuring the alignment between the features on both sides of the grating is difficult due to the small feature sizes and the relatively large separation distance between the two sets of gratings. This paper provides details on our fabrication approach, the geometries of the gratings obtained, and measurements on the alignment accuracy of the features on both sides of the substrate.

Experimental Details

In this work, a 140 μm deep, 1.95 μm wide, and 3.91 μm pitch Si phase grating was fabricated by aligning and etching 70 μm deep grating features on both sides of a Si wafer aligned within 0.5 μm. Our integration approach for accommodating these challenges is illustrated in Figure 1. The work presented in this paper provides details and results from 1(a) through 1(d). To extend this approach to creating an analyzer grating, we can employ a process developed in previous

work [5] and deposit a conformal platinum (Pt) plating seed metal by atomic layer deposition (ALD), 1(e), followed by precision electrodeposition of gold (Au), 1(f).

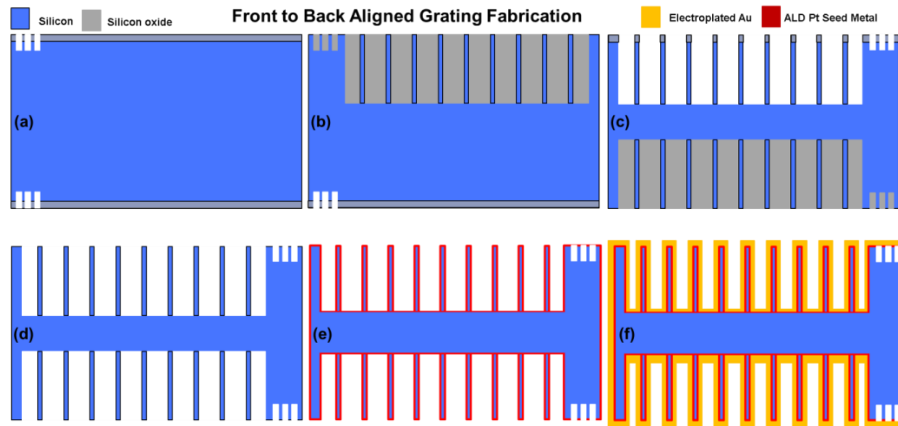

Figure 1: Integration approach for front to back aligned XPCI gratings. (a) Align, pattern and etch front and backside alignment marks. (b) Etch topside Si grating and fill with oxide to support fragile Si bars. (c) Flip substrate, pattern and etch backside Si grating. (d) Selectively etch oxide. (e) Deposit conformal ALD Pt seed metal. (f) Precision electrodeposit Au on top of Pt seed.

The front-to-backside alignment approach utilizes a Nikon^{TM} microelectronics lithography stepper system (model il2) capable of aligning features on the opposite side of the wafer to within 0.5 µm. The preferred front-side alignment method, field image alignment (FIA), measures several marks on the wafer surface using video signals from an optical microscope above the front side of the wafer and a grid is calculated for accurate placement of each shot with accuracies as low as 0.15 µm. The back-side alignment method (BS-FIA) works similarly, except that the video signals for this alignment come from miniature video cameras embedded three positions in the wafer holder. The backside cameras are immobile and positioned in three locations to obtain X, Y, and theta alignment. The magnification of the mark signals obtained from these backside cameras is low therefore it is critical to obtain as much contrast between the BS-FIA marks and the surrounding substrate surface as possible in order to achieve the optimum front-to-backside alignment. Obtaining high contrast in the BS-FIA signal is achieved by first depositing 0.5 µm of thermal oxide on both side of the Si wafer. Two sequential reactive ion etches are used to etch through the oxide and 3-4 µm into the Si. The 0.5 µm thick SiO_2 layer creates a darker reflection of light back into the BS-FIA camera system while the bottom of the DRIE etched Si is smooth and has high reflectivity creating bright features. The BS-FIA and FIA marks are patterned on the front side of the substrate with the BS-FIA marks patterned at the observation positions of the stage and the FIA marks patterned at the edge of the wafer outside the grating area. Similarly, FIA marks are patterned on the backside of the wafer at the periphery of the wafer, aligned to the to the BS-FIA marks on the front side of the wafer.

Once the alignment marks are etched, a 2 µm thick PETEOS SiO_2 hard mask is deposited on the front side of the wafer. This PETEOS film also protects the BS-FIA marks from chuck damage

while processing on the opposite side of the substrate. The maximum imaging field of the stepper is smaller than the desired area of the final grating so a the 14000 µm by 14001 µm patterned area is stitched across a 150 mm diameter wafer creating a 7 x 7 array resulting in a final grating area of 96 cm^2. The reticle area is filled with 1.555 µm wide grating features on a 3.91 µm pitch. The 3.91 µm pitch was determined based on the separation distance between the source grating and phase grating. The 1.555 µm wide open features in the resist are biased to compensate for lateral etching during the DRIE in order to achieve a resultant 50% duty cycle (1.955 µm Si feature on a 3.91 µm pitch). The lateral alignment between each stitched column is aligned within the 0.15 µm tolerance of the FIA alignment system. The vertical alignment can be overlapped between each stitched area and an overlap of 1 µm is used to relax the vertical stitching tolerance. Once the front side stitched pattern is developed, the 2.5 µm thick SiO_2 hard mask is etched, followed by a 70 µm deep Si etch. Prior to patterning the backside of the wafer, a 2 µm thick LPCVD TEOS film is deposited coating the front side of the wafer to protect the fragile grating features as well as the backside of the wafer, serving as a SiO_2 hard mask for the backside Si etch. Images of the front side Si gratings after the SiO_2 deposition are shown in Figure 2. The LPCVD TEOS deposition joins at the top of the gratings features to support the Si bars, but it does not completely fill the grating.

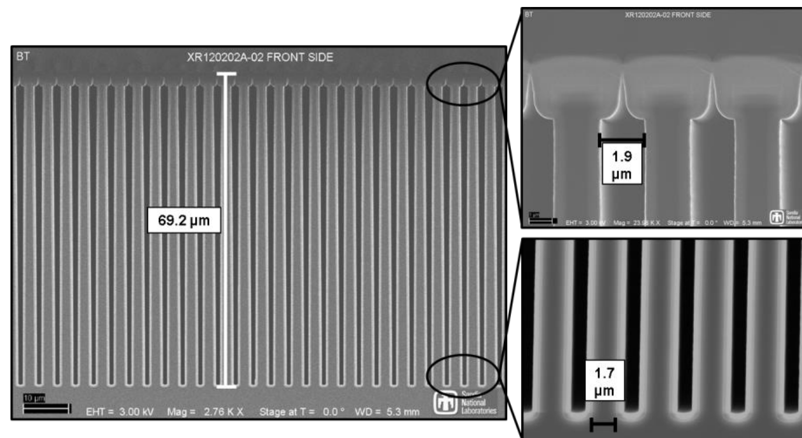

Figure 2: Front side Si grating etched 69.2 um into Si with DRIE and subsequent LPCVD TEOS deposition to support the grating features while processing on the opposite side of the substrate.

An etch depth of 70 µm was targeted and an actual depth of 69.2 µm was achieved. The biased 1.55 µm features were slightly under biased resulting in slightly less than a 50% duty cycle. The substrate is then flipped upside down and the backside gratings are aligned to the FIA marks that were patterned at the periphery of the wafer backside. Similarly, the 2.5 µm thick SiO_2 hard mask is etched followed by a 70 µm deep Si etch. Figure 3 shows cross section SEM images of the backside gratings. The inset image in Figure 3 shows the remaining oxide hard mask at the top of the grating feature illustrating the amount of lateral etch that results from the DRIE process, again with a slight undercompensated bias in the lithographic dimension of the Si feature which can be adjusted in future iterations.

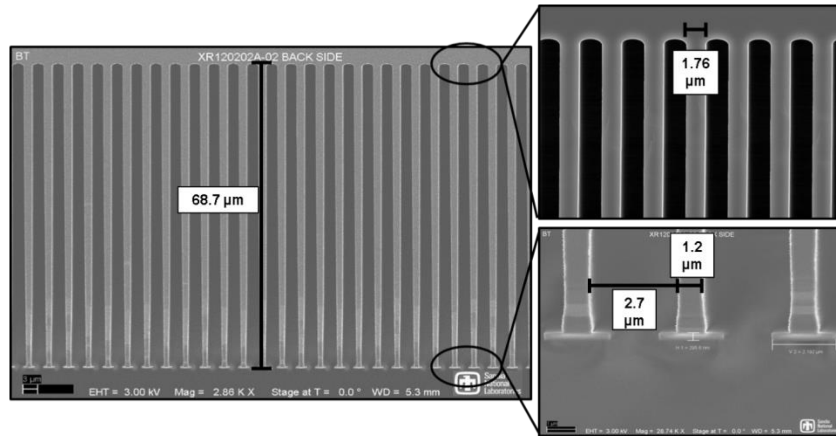

Figure 3: Cross section SEM image of the backside Si gratings prior to removing the oxide hard mask.

After the grating features are etched on both sides of the substrate, the support oxide on the front side and the hard mask oxide on the backside of the wafer must be removed. A selective wet etch in dilute hydrofluoric acid (HF) and a dry chemical etch in vapor HF (VHF) were used to remove the SiO_2. At first attempts, the wet HF etch was performed and then the wafers were air dried after rinsing with DI water and IPA. The surface tension of the liquid during drying pulled the Si bars together and resulted in damaged features. Figure 4 shows optical microscope images of the gratings prior to the oxide removal, (a), as well as optical images after the wet etch and air dry where damage is seen at some of the Si bars as a result of surface tension, (b).

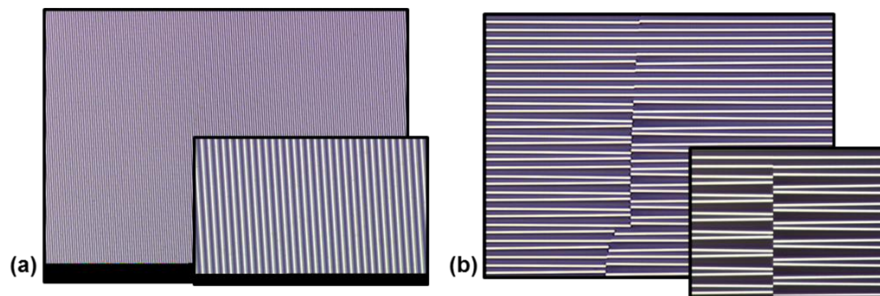

Figure 4: optical microscope images of the Si grating prior to (a) and after (b) removing the oxide and allowing the wafer to dry in air after an IPA rinse. Damage is seen on some of the Si bars as a result of surface tension during the drying process.

A critical point dryer was used to avoid the damaging surface tension forces and successfully resulted in undamaged Si gratings. After the wet HF release, the wafer is rinsed to 12 Mohm resistivity and then a 30% H_2O_2 solution is used to re-grow a very thin layer of SiO_2 to create a hydrophilic surface on both sides of the wafer. The wafer is then submersed in isopropyl alcohol and transferred to a critical point dryer. Both optical and cross-sectional SEM images of a wafer after the oxide remove and critical point dryer was used are shown in Figure 5.

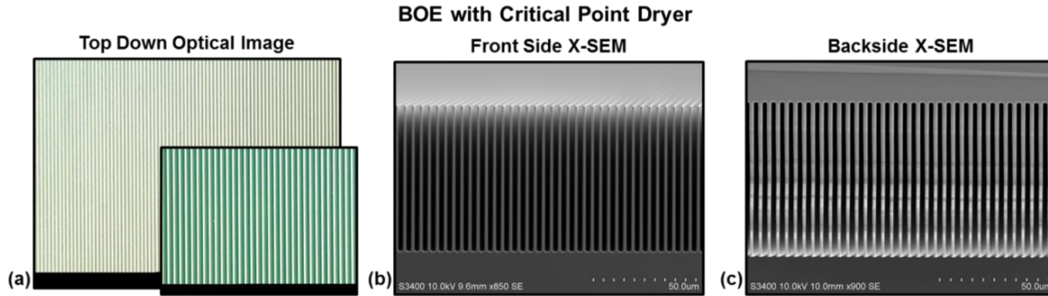

Figure 5: (a) optical and cross section SEM images of the (b) front side and (c) backside Si gratings after removing the oxide in a wet HF chemistry and drying the wafer with a critical point dryer. No damage to the Si bars was detected when the critical point dryer was used. The striations in (c) are the result of an un-even cleave through the substrate.

As an alternative approach to the wet SiO_2 etch, a VHF tool was used as a dry oxide etch bypassing the surface tension issues all together. The 150 mm diameter wafer is supported by three pins positioned in an equilateral triangle 10 mm from the edge of the wafer and outside of the active area of the grating. The VHF is highly selective in etching oxide and not attacking Si. Figure 6 shows top down optical images of the grating area as well as cross section SEM images of the front and backside grating.

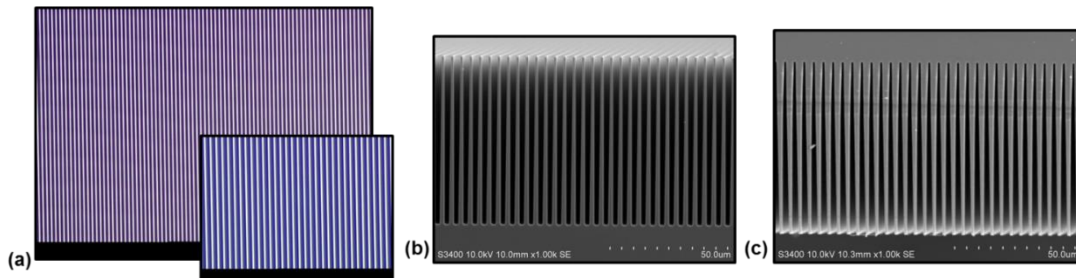

Figure 6: (b) optical and cross section SEM images of the (b) front side and (c) backside Si gratings utilizing a dry VHF oxide etch.

Results and Discussion

After fabricating these gratings with features etched and aligned on both sides of the substrate, we attempted to quantify the alignment accuracy of the Nikon BS-FIA system. We first attempted this measurement with cross-sectional SEM imaging and the results are shown in Figure 7. Using the SEM measurement software, vertical lines were drawn on the SEM image to try and correlate the alignment between two corresponding features on both sides of the substrate. Qualitatively the SEM measurement shows that the two features are well aligned however, it was not possible to quantify the alignment precision using this technique because the 1.95 µm wide features are separated by a distance that is more than two orders of magnitude larger (535 µm) than the dimension of the features.

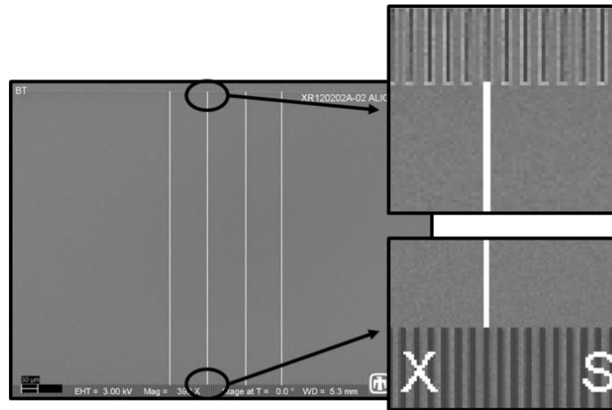

Figure 7: Cross sectional SEM images in an attempt to quantify the front to backside alignment accuracy. Use of an SEM to measure alignment accuracy is unable to obtain the measurement accuracy which we need to quantify the alignment between front and backside features.

A Zeiss Xradia 520 Versa NanoCT system was also used to try and characterize the front-to-back alignment accuracy. The pitch of two aligned features were measured in the CT scan on both the front side and the backside of the substrate and are shown in Figure 8. The positions of these measurements were measured from the same distance from the edge of the Si grating, 10 µm, in order to remove any error in the pitch measurement due to the slightly angled etch profile of the Si grating. The measurements obtained from the nanoCT system show that the two features are aligned within 0.5 µm of one another; however, one pixel in the nanoCT system is 0.5 µm so we are unable to statistically quantify the alignment accuracy of the measurement. We have reached an inherent physical limitation in being able to quantify the alignment accuracy because the tolerance we are attempting to measure is less than 0.5 µm and the separation distance is three orders of magnitude higher, 0.5 mm. Qualitatively we are confident that the two features are aligned within 0.5 µm of one another.

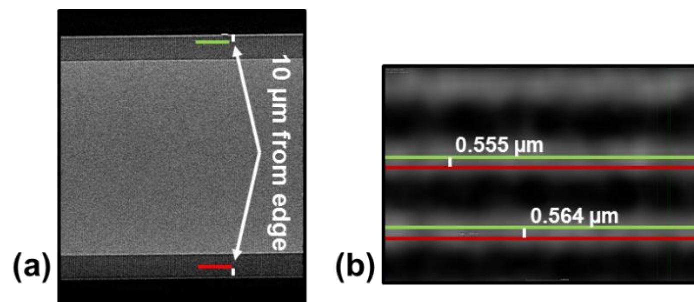

Figure 8: NanoCT measurements attempting to measure alignment accuracy between front and backside features. These measurements qualitatively confirm that we're within 0.5 um alignment accuracy. (a) side view CT scan of BSA gratings and (b) superimposed pitch measurements.

Conclusion

In this work we have investigated the feasibility of aligning and fabricating XPCI gratings on both sides of a substrate. Utilizing backside alignment capabilities of a lithographic stepper we

have achieved a 3.91 µm period phase grating that is 140 µm deep (70 µm on each side of the substrate). This dual sided grating fabrication methodology effectively doubles the aspect ratio of the final grating and can be combined with any other grating fabrication approach such as LIGA, anisotropic KOH etch, or MACE. Doubling the thickness of the grating opens the possibility of using cost effective materials to replace the commonly used Au absorbing material and obtain the same contrast in the x-ray signal or alternatively allows higher x-ray source energies to be used, opening up a new material set to be analyzed using XPCI. In future work, we are combining this double sided DRIE grating approach with precision Au electrocoating to realize large field of view analyzer gratings for high energy XPCI.

Acknowledgements

Supported by the Laboratory Directed Research and Development program at Sandia National Laboratories, a multimission laboratory managed and operated by National Technology and Engineering Solutions of Sandia, LLC., a wholly owned subsidiary of Honeywell International, Inc., for the U.S. Department of Energy's National Nuclear Security Administration under contract DE-NA-0003525.

References

[1] J. Mohr, T. Grund, D. Kunka, J. Kenntner, J. Leuthold, and J. Meiser, High Aspect Ratio Gratings for X-Ray Phase Contrast Imaging. International Workshop on X-Ray and Neutron Phase Imaging with Gratings 1466 (2012) 41-50.

[2] T. J. Chroter, F. Koch, P. Meyer, M. Baumann, D. Munch, D. Kunka, S. Engelhardt, M. Zuber, T. Baumbach, J. Mohr, Large area gratings by x-ray LIGA dynamic exposure for x-ray phase-contrast imaging, J. of Micro/Nanolithography, MEMS, and MOEMS, 16(1), 013501 (2017).

[3] L. Romano, J. Vila-Comamala, M. Kagias, K. Vogelsang, H. Schift, M. Stampanoni, K. Jefimovs, High aspect ratio metal micrcasting by hot emboxxing for X-ray optics fabrication, Microelectronic Engineering 176 (2017) 6-10.

[4] C. Gunzweig, F. Pfeiffer, O. Bunk, T. Donath, G. Huhne, G. Frei, M. Dierolf, and C. David, Design, fabrication, and characterization of diffraction gratings for neutron phase contrast imaging, Review of Scientific Instruments 79, 053703 (2008).

[5] A. E., Hollowell, C. L. Arrington, J. J. Coleman, P. S. Finnegan, A. M. Rowen, and A. L. Dagel, Extensively long high aspect ratio gold analyzer gratings , X-ray and Neutron Phase Imaging with Gratings (2015).

[6] C. Chang and A. Sakdinawat, Ultra-high aspect ratio high-resolution nanofabrication for hard X-ray diffractive optics, Nature Communications, 10.1038/ncomms5243.

[7] M. Vangbo and Y. Backlund, Precise mask alignment to the crystallographic orientation of silicon wafers using wet anisotropic etching, Journal of Micromechanics and Microengineering, 6 (1996) 279-284.

[8] J. H. han, S. Radhakrishnan, and C-H. Lee, A novel batch-processing method for accurate crystallographic axis alignment, Journal of Micromechanics and Microenginerring, 23 (2013 055017.

[9] H. Jansen, M. de Boer, R. Wiegerink, N. Tas, E. Smulder, C. Neagu, and M. Elwenspoek, RIE lab in high aspect ratio trench etching of silicon, Microelectronic Engineering 35 (1997) 45-50.